Article:
Yağmuroğlu, İ, Ozdemir, Z. and Askes, H. orcid.org/0000-0002-4900-1376 (2023) Spatial and temporal averaging in the homogenisation of the elastodynamic response of periodic laminates. European Journal of Mechanics - A/Solids, 100. 104973. ISSN 0997-7538

https://doi.org/10.1016/j.euromechsol.2023.104973

European Journal of Mechanics / A Solids 100 (2023) 104973

Contents lists available at ScienceDirect

European Journal of Mechanics / A Solids

journal homepage: www.elsevier.com/locate/ejmsol

Spatial and temporal averaging in the homogenisation of the elastodynamic response of periodic laminates

İrem Yağmuroğlu [a], Zuhal Ozdemir [a], Harm Askes [a,b,*]

[a] Department of Civil and Structural Engineering, University of Sheffield, United Kingdom
[b] Faculty of Engineering Technology, University of Twente, The Netherlands

ARTICLE INFO

Keywords:
Multi-scale modelling
Hill–Mandel Principle
Homogenisation
Space–time averaging
Representative Volume Element
Wave propagation

ABSTRACT

This paper suggests a methodology to obtain homogenised material properties from a transient dynamic numerical model. The standard Hill–Mandel Principle, based on spatial averages, is extended with time averaging. Thus, in addition to a sufficiently large Representative Volume Element (RVE) to carry out the averaging in space, a sufficiently large time window is required to carry out the time averaging. The space–time averaging procedure is validated for a periodic laminate bar subjected to a variety of boundary conditions, impedance contrasts and loading conditions. The homogenised results converge to the analytical solutions and confirm that having a higher impedance contrast between laminate components requires not only larger RVE sizes but also longer time averaging windows. The most efficient macroscopic approximation is obtained by a balanced increase in RVE size and time averaging window.

1. Introduction

Composite materials are widely used due to their multi-scale character so that the benefits of both coarse-scale (structure level) and fine-scale (constituent level) can be exploited to obtain enhanced mechanical properties such as stiffness, damping, strength and thermal conductivity to meet various requirements of engineering applications (Herakovich, 2012; Kanouté et al., 2009). For a wide range of engineering problems, composites are often modelled as homogeneous materials without considering their microstructure (Kouznetsova et al., 2004). However, due to wave dispersion, composite materials do not behave the same way as their homogeneous counterparts under dynamic excitations. In particular, microstructural effects have a significant impact on material behaviour at high loading rates (Wang and Sun, 2002). Moreover, composite materials exhibit different mechanical behaviour at different levels depending on their multi-scale structures so that this size effect is required to be captured by their multi-scale models (Zhu et al., 1997). Therefore, an effective material model of a composite captures their mechanical behaviour accurately at different scales.

Various multi-scale modelling approaches have been developed over the years due to an interest in predicting the mechanical behaviour of composite materials considering their multi-scale behaviour for engineering practice (Weinan et al., 2007; Nguyen et al., 2011; Pham et al., 2013). The use of the direct simulation method, whereby every microstructural detail is modelled separately and explicitly, for modelling composite materials with microstructures requires enormous computational effort and cost. As an alternative, the principle of separation of length scales (given by $\ell \ll L$, where ℓ represents the length of microstructure, whereas L represents the length of macrostructure as depicted in Fig. 1) allows for saving costs by averaging microscopic problems for the overall behaviour of composite materials. For example, heterogeneous multi-scale methods may combine molecular dynamics for micro-scales with continuum mechanics for macro-scales to model advanced characteristics of composite materials. Thus, multi-scale methods may be employed for predicting complex microstructural material behaviour and designing new composite materials.

In multi-scale methods, consistency between micro- and macro-scales is achieved by the averaging theorems and homogenisation methods. The pioneering micro–macro averaging method, the Hill–Mandel Principle of Macrohomogeneity, is only valid when separation of scales can be assumed (Hill, 1963, 1972). The theory of micro–macro averaging is set up by the spatial volume average of microscopic virtual work with respect to the virtual work of a macroscopic material point. As such, heterogeneities in a microstructure are averaged to reflect effective overall properties in a macrostructure. Classical micro–macro averaging methods have been implemented to predict the material behaviour of composites, when micro-inertia and non-local effects are negligible (Willis, 1981; Hashin, 1983; Nemat-Nasser, 1999). In statics, the micro–macro averaging method enables the stress and strain averaging of the micro-scale to represent constitutive behaviour on the macro scale. In other words, macroscopic effective material quantities

* Corresponding author at: Faculty of Engineering Technology, University of Twente, The Netherlands.
E-mail address: h.askes@utwente.nl (H. Askes).

https://doi.org/10.1016/j.euromechsol.2023.104973
Received 3 October 2022; Received in revised form 7 March 2023; Accepted 12 March 2023
Available online 15 March 2023

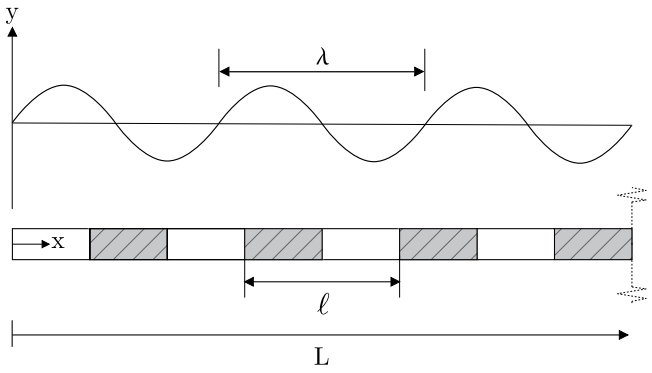

Fig. 1. Spatial length parameters for a laminate.

are extracted from the result of associated microscopic boundary value problems. These averaged macroscopic quantities rely exclusively on the quality of an associated microscopic model. Accordingly, the microstructure boundary value problem must be solved, e.g. by using a finite element model.

In the classical work of multi-scale modelling, a microstructural model can be described as the representation of microheterogeneity of the material. The concept of representative volume element (RVE) is applied to predict the material behaviour of a heterogeneous microstructure (Gitman et al., 2005; Kouznetsova et al., 2004). An RVE is a microstructural model of the material that has finite dimensions. The RVE size, denoted as L_{m}, should be large enough to encapsulate all microscopic features as a representation of a macroscopic model and, at the same time, as small as possible to save computational cost. The identification and quantification of the RVE are important issues in multi-scale modelling problems. Several analytical, numerical and experimental studies have been performed to identify and quantify RVEs in statics and dynamics (Drugan and Willis, 1996; Ostoja-Starzewski, 2001; Kanit et al., 2003). In statics, even though the RVE size can be defined statistically for linear-elastic and hardening material behaviour, the RVE was demonstrated not to exist when the material is in the softening regime, because strain localisation implies separation of scales is no longer applicable (Gitman et al., 2007). The RVE is determined by geometric and material properties of the microstructure so that the periodicity of both material and boundary conditions should be considered. In the context of the periodicity of material, the RVE size of periodic microstructures certainly is equal to the size of a microstructural unit cell ℓ. However, it is more challenging to determine a RVE for random microstructures (Gitman et al., 2006). On the other hand, the RVE size with periodic boundary conditions was demonstrated to be smaller than the RVE size with non-periodic boundary conditions. In addition, the influence of periodicity in material and boundary conditions on the RVE size varies depending on the loading conditions (Gitman et al., 2007).

In dynamics, the increasing interest in advanced engineering applications such as band gaps and acoustic metamaterials has highlighted the importance of wave propagation phenomena in composite materials (Sheng and Chan, 2005; Sridhar et al., 2020). In the context of multi-scale modelling, averaging and homogenisation methods have been developed to incorporate inertia effects and body forces in order to model wave behaviour of composite materials subjected to dynamic excitations (Nemat-Nasser and Hori, 2013; Chen and Fish, 2000; Wang and Sun, 2002; Nassar et al., 2015; Fish et al., 2012). Methods formulated in the frequency domain have become popular due to the increase in the use of acoustic metamaterials and phononic crystals, yet the frequency domain can be only applicable for linear elastic materials and periodic microstructures (Srivastava and Nemat-Nasser, 2014; Srivastava, 2015; Sridhar et al., 2018). Accordingly, multi-scale methods based on the time domain are more comprehensive for general cases (e.g. complex time-dependent boundary conditions) (Pham et al., 2013). The modelling of transient interactions and micro-inertia effects in space and time implies that the wavelength of applied excitations needs to be considered in addition to the size of microstructure and macrostructure. Therefore, for dynamic problems, three physical length parameters are involved in total, as shown in Fig. 1. When the shortest wavelength in the initial disturbance λ is much larger than the size of the microstructure ℓ and the size of the structure L is much larger than its microstructure ℓ, the response can be assumed as a homogeneous material behaviour on the macro level. As a result, the RVE-based multi-scale problem can be solved by the classical quasi-static homogenisation formulations. Conversely, when the wavelength approaches the size of microstructure, wave dispersion becomes significant and must be modelled by averaging theorems with effective constitutive relations that account for the dynamic response of the material. Similar to statics, RVE-based multi-scale modelling has been widely implemented in dynamics for the contribution of micro-inertia and body forces (de Souza Neto et al., 2015). However, the size of RVE in statics is not necessarily equal to the size of RVE in dynamics due to the dispersive behaviour resulting from the reflection and refraction of the wave. Therefore, the RVE size in dynamics should be determined separately to obtain accurate averaging between micro and macrostructure. For a periodic laminate, the size of RVE in dynamic was argued to be larger than the unit cell size and dependent on the component properties (Bennett et al., 2007). Moreover, a higher contrast in the component properties, thus exhibiting more dispersive behaviour, was shown to lead to increase in the RVE size (Bagni et al., 2015).

The classical Hill–Mandel Principle of Macrohomogeneity as used in statics concerns only micro–macro averaging in space. However, in dynamics macro and micro-scale variables are affected by temporal fluctuations as well as spatial fluctuations. Several extensions of the Hill–Mandel Principle theorems have been recently proposed for the micro–macro averaging in dynamics, including micro-inertia and body forces (Reina Romo, 2011; Pham et al., 2013; de Souza Neto et al., 2015). In particular, Reina Romo (2011) discusses homogenisation in dynamics with the option to apply averaging in time as well as in space. As explained by Reina Romo (2011), time averaging is equivalent to assuming the principle of separation of time scales, in addition to the principle of separation of length scales. It is this concept of time averaging that we aim to explore further in this paper. When time averaging is considered in addition to space averaging, a relevant question arises: what is the time window over which time averaging should be carried out?

As a matter of principle, in RVE-based multi-scale problems, taking microstructural sample sizes larger than the RVE size should not have an impact on the response of the macrostructure. Extending this principle to the time dimension, a time window for averaging should be selected such that taking a larger window would not affect the homogenised macroscopic response. In this paper, we will explore how to select this time window for time averaging, and how it relates to the RVE size that is used for the averaging in space.

An extended version of the Hill–Mandel Principle of macro-homogeneity is implemented with the finite element method to investigate the influence of the RVE size and time averaging window in dynamics. The micro-to-macro transition is carried out by averaging in space and time. With this setup, the influence of RVE size and time averaging window can be investigated to obtain the most accurate predictions for the macro-structural properties. In particular, by focussing on a laminated bar with one spatial dimension, it will be possible to assess whether it is possible to trade off RVE size against length of the time averaging interval, and vice versa. The analysis is repeated for various boundary conditions, a number of material parameter sets and different loading regimes to test the sensitivity of the findings.

2. Micro–macro averaging

In this section, a new micro–macro averaging model is developed for use within the finite element method to predict the size of RVEs in space and time based on the mechanical behaviour of periodic microstructures. Briefly, space–time averaging can be achieved in three main stages. First, the micro boundary value problem is defined and solved within a finite element framework. Then, the micro–macro coupling is established between macroscopic strain and microscale displacement on the boundary, and also between macroscopic stress and microscale tractions. Finally, the space and time-averaging methods are employed to obtain the homogenised material properties. In order to enable consistent comparison of computational effort, a finite element discretisation is employed with a lumped mass matrix and the Central Difference explicit time integrator so that the computational costs scale linearly with the resolution of both the spatial and time dimension.

2.1. Space averaging

The static averaging approach enables a macroscopic integration point response to be replaced by its microscopic counterpart obtained by integrating over the size of the RVE. The volume average of the RVE stress field subjected to the local macroscopic strain tensor defined as prescribed displacement or traction is established for energy consistency between micro and macrostructures. First, the microscopic boundary value problem is defined. In the absence of body forces, the RVE dynamic equilibrium at any point is expressed as:

$$\frac{\partial}{\partial x}\sigma_{\mathrm{m}} - \dot{p}_{\mathrm{m}} = 0 \tag{1}$$

where σ_{m} is the microscale stress and p_{m} is the microscale linear momentum which are given by the following equations

$$p_{\mathrm{m}} = \rho_{\mathrm{m}}\,\dot{u}_{\mathrm{m}} \tag{2}$$

$$\sigma_{\mathrm{m}} = E_{\mathrm{m}}\,\varepsilon_{\mathrm{m}} \tag{3}$$

where ρ_{m} and E_{m} are the microstructural mass density and Young's modulus, respectively. The microstructural boundary value problem is solved for each RVE. The material behaviour is determined by the obtained kinematic quantities, the microscopic velocity $\dot{u}_{\mathrm{m}}$, where a dot indicates the derivative of displacement u_{m} with respect to time, and the microscopic strain ε_{m}. In statics, for the micro–macro relations, the total variation of work on the macro-level is equal to the volume average of the variation work on the micro-level, which is given by (Hill, 1963)

$$\sigma_{\mathrm{M}}\,\varepsilon_{\mathrm{M}} = \frac{1}{V_{\mathrm{m}}}\int_{V_{\mathrm{m}}}\sigma_{\mathrm{m}}\,\varepsilon_{\mathrm{m}}\,\mathrm{d}V_{\mathrm{m}} \tag{4}$$

where σ_{M} and ε_{M} are macroscopic stress and strain, respectively, and V_{m} is the volume of the microstructure. The macro deformation tensor ε_{M} can be linked in the associated RVE to the position $x_{\mathrm{i}} = \varepsilon_{\mathrm{M}} x_{0\mathrm{i}}$. Here, i and $x_{0\mathrm{i}}$ represents any point and initial position in the RVE, respectively. This shows how the macroscale quantities can be obtained by the integration of micro kinematic quantities in the RVE. Consequently, the macro stress σ_{M} and the macro strain ε_{M}, respectively, can be obtained by decomposing Eq. (4), presented as the volume-averages of the microscale quantities

$$\langle\sigma_{\mathrm{m}}\rangle_x = \frac{1}{V_{\mathrm{m}}}\int_{V_{\mathrm{m}}}\sigma_{\mathrm{m}}\,\mathrm{d}V_{\mathrm{m}} \tag{5}$$

$$\langle\varepsilon_{\mathrm{m}}\rangle_x = \frac{1}{V_{\mathrm{m}}}\int_{V_{\mathrm{m}}}\varepsilon_{\mathrm{m}}\,\mathrm{d}V_{\mathrm{m}} \tag{6}$$

where $\langle\cdot\rangle_x$ denotes the spatial averaging operator implied by the previous two expressions. Upscaling, a transition from micro to macroscale, is implemented based on the Hill–Mandel Principle in order to transfer both static and dynamic features of heterogeneity to a macro-level. Namely, inertia effects on the micro-level are transferred alongside the stresses to the macro-level through upscaling, so dynamic effects on macro-level are generated depending on a microstructure. In addition to the work of strain, the work of acceleration is added into the variation of work performed on both scales so that the Hill–Mandel condition in dynamics is written as (Hill, 1963)

$$\sigma_{\mathrm{M}}\,\delta\varepsilon_{\mathrm{M}} + \frac{d}{dt}p_{\mathrm{M}}\,\delta u_{\mathrm{M}} = \frac{1}{V_{\mathrm{m}}}\int_{V_{\mathrm{m}}}\sigma_{\mathrm{m}}\,\delta\varepsilon_{\mathrm{m}}\,\mathrm{d}V_{\mathrm{m}} + \frac{1}{V_{\mathrm{m}}}\int_{V_{\mathrm{m}}}\frac{d}{dt}p_{\mathrm{m}}\,\delta u_{\mathrm{m}}\,\mathrm{d}V_{\mathrm{m}} \tag{7}$$

where p_{m} and p_{M} are microscopic and macroscopic momentum, respectively. Upscaling relations can be obtained from Eq. (7). The averaged momentum and velocity by microscopic quantities can be written as

$$\langle p_{\mathrm{m}}\rangle_x = \frac{1}{V_{\mathrm{m}}}\int_{V_{\mathrm{m}}}p_{\mathrm{m}}\,\mathrm{d}V_{\mathrm{m}} \tag{8}$$

$$\langle v_{\mathrm{m}}\rangle_x = \frac{1}{V_{\mathrm{m}}}\int_{V_{\mathrm{m}}}v_{\mathrm{m}}\,\mathrm{d}V_{\mathrm{m}} \tag{9}$$

2.2. Time averaging

In this section, time averaging will be added to develop the dynamic energy averaging relation. The space averaging in micro-to-macro transition is extended to account for the time averaging. This transition requires the application of an additional time-dependent averaging, which can be considered as an extended version of the Hill–Mandel Principle. Apart from the effect of spatial variability in the microstructure, the time averaging comprises the time history of the wave propagation through the microstructure. Thus, time and history-dependent stress–strain and momentum–velocity relationships are both transferred to the macro-level to improve the accuracy and reliability of the homogenised material behaviour. The suggested procedure is to extend the coupling between micro and macro scales by integrating the Hill–Mandel Principle in time, that is

$$\begin{aligned}\sigma_{\mathrm{M}}\delta\varepsilon_{\mathrm{M}} + \frac{d}{dt}p_{\mathrm{M}}\delta u_{\mathrm{M}} = {}& \frac{1}{T_{\mathrm{m}}}\frac{1}{V_{\mathrm{m}}}\int_{t_0}^{t_f}\int_{V_{\mathrm{m}}}\sigma_{\mathrm{m}}\delta\varepsilon_{\mathrm{m}}\,\mathrm{d}V_{\mathrm{m}}\mathrm{d}t_{\mathrm{m}} \\ & + \frac{1}{T_{\mathrm{m}}}\frac{1}{V_{\mathrm{m}}}\int_{t_0}^{t_f}\int_{V_{\mathrm{m}}}\frac{d}{dt}p_{\mathrm{m}}\delta u_{\mathrm{m}}\,\mathrm{d}V_{\mathrm{m}}\mathrm{d}t_{\mathrm{m}}\end{aligned} \tag{10}$$

where $T_{\mathrm{m}} \equiv t_f - t_0$ is the time period of total propagation of a wave on the micro level and t_0 is the initial time, t_f is the final time. Analogous to space averaging, the time averaged quantities can be obtained from Eq. (10) as

$$\langle\langle\sigma_{\mathrm{m}}\rangle_x\rangle_t = \frac{1}{T_{\mathrm{m}}}\frac{1}{V_{\mathrm{m}}}\int_{t_0}^{t_f}\int_{V_{\mathrm{m}}}\sigma_{\mathrm{m}}\,\mathrm{d}V_{\mathrm{m}}\,\mathrm{d}t_{\mathrm{m}} \tag{11}$$

$$\langle\langle\varepsilon_{\mathrm{m}}\rangle_x\rangle_t = \frac{1}{T_{\mathrm{m}}}\frac{1}{V_{\mathrm{m}}}\int_{t_0}^{t_f}\int_{V_{\mathrm{m}}}\varepsilon_{m}\,\mathrm{d}V_{\mathrm{m}}\,\mathrm{d}t_{\mathrm{m}} \tag{12}$$

$$\langle\langle p_{\mathrm{m}}\rangle_x\rangle_t = \frac{1}{T_{\mathrm{m}}}\frac{1}{V_{\mathrm{m}}}\int_{t_0}^{t_f}\int_{V_{\mathrm{m}}}p_{\mathrm{m}}\,\mathrm{d}V_{\mathrm{m}}\,\mathrm{d}t_{\mathrm{m}} \tag{13}$$

$$\langle\langle v_{\mathrm{m}}\rangle_x\rangle_t = \frac{1}{T_{\mathrm{m}}}\frac{1}{V_{\mathrm{m}}}\int_{t_0}^{t_f}\int_{V_{\mathrm{m}}}v_{\mathrm{m}}\,\mathrm{d}V_{\mathrm{m}}\,\mathrm{d}t_{\mathrm{m}} \tag{14}$$

where $\langle\cdot\rangle_t$ denotes the temporal averaging operator and $\langle\langle\sigma_{\mathrm{m}}\rangle_x\rangle_t$, $\langle\langle\varepsilon_{\mathrm{m}}\rangle_x\rangle_t$, $\langle\langle p_{\mathrm{m}}\rangle_x\rangle_t$, and $\langle\langle v_{\mathrm{m}}\rangle_x\rangle_t$ are the space and time averaged stress, strain, momentum and velocity, respectively. As a result of the space–time averaged stress–strain and momentum-velocity relationships, the transition material parameters for the macro-level are given by

$$E_{\mathrm{M}} = \langle\langle\sigma_{\mathrm{m}}\rangle_x\rangle_t / \langle\langle\varepsilon_{\mathrm{m}}\rangle_x\rangle_t \tag{15}$$

$$\rho_{\mathrm{M}} = \langle\langle p_{\mathrm{m}}\rangle_x\rangle_t / \langle\langle v_{\mathrm{m}}\rangle_x\rangle_t \tag{16}$$

where E_{M} and ρ_{M} are the time–space averaged Young's modulus and mass density on the macro level, respectively. The micro–macro averaging model is employed for each macroscopic integration point to describe the homogenised macroscopic behaviour underlying microscopic heterogeneous behaviour.

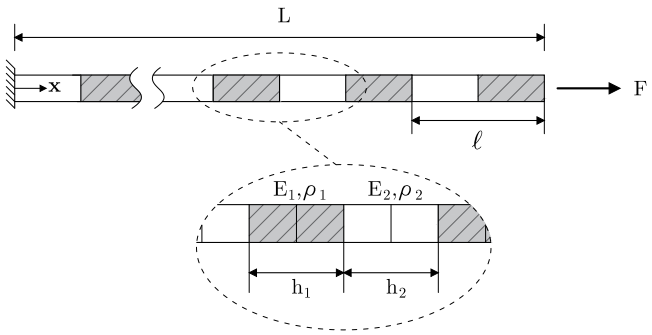

Fig. 2. A periodically laminated bar.

Remark 1. The micro–macro averaging model has been verified not to be affected by the order of averaging since all involved processes are linear. Although not shown in this paper, the macroscale parameters obtained using first the space averaging and then the time averaging were found to be the same as the parameters obtained in the opposite order of averaging operations. In this paper, the former order is employed in the numerical examples.

3. Numerical results

We present several numerical examples to assess the convergence of the microstructure size in which spatial and temporal fluctuations become insignificant and the macroscopic response can be approximated by the averaged microscopic response. The macroscopic response of a one-dimensional laminate bar shown in Fig. 2 is investigated under various loading and boundary conditions. The bar is restrained at the left end and subjected to several loading conditions at the other end (e.g. constant and harmonic loads). The finite element model consists of periodic unit cells, each discretised with four linear elements with length h. The bar length varies based on the number of unit cells, which each have a length of 1 m and a cross-sectional area of 1 m^2. The central difference method for time integration is used with a time step size of 0.1 s.

A unit cell consist of two layers, the constitutive parameters of which are Young's modulus E_1 and E_2, mass densities ρ_1 and ρ_2, elastic impedances $z_1 = \sqrt{E_1\rho_1}$ and $z_2 = \sqrt{E_2\rho_2}$, and wave speeds $c_1 = \sqrt{E_1/\rho_1}$ and $c_2 = \sqrt{E_2/\rho_2}$. While the material properties of two laminate elements are chosen for three levels of the impedance contrast $z_1/z_2 = 10$, $z_1/z_2 = 100$ and $z_1/z_2 = 1000$, the wave speeds are kept the same between the components of laminate, in particular $c_1 = c_2 = 1$ m/s.

In the numerical examples, the RVE is determined by user defined parameters, which are the number of unit cells N_{uc} and the number of wave propagations N_{wp}. For the laminate bar, the RVE size is equivalent to the bar length selected as N_{uc} times ℓ. Moreover, the laminate bar is loaded for duration t_f, where t_f is found by dividing the bar length by the wave speed, times a factor N_{wp}. At time $t = t_f$, the stresses, strains, velocities and momentum values are sampled and averaged in space and time. The macroscopic material properties are validated against the analytical exact solutions of the effective Young's modulus E_{avr} and the effective mass density ρ_{avr} obtained for periodic composites (Fish and Chen, 2001; Andrianov et al., 2008) as follows

$$E_{\text{avr}} = \frac{E_1 E_2}{(1-\alpha)E_1 + \alpha E_2} \tag{17}$$

$$\rho_{\text{avr}} = \alpha\rho_1 + (1-\alpha)\rho_2 \tag{18}$$

where $0 \leq \alpha \leq 1$.

3.1. Effect of boundary conditions

In order to establish appropriate boundary requirements for the space–time averaging model, we firstly adopt Dirichlet conditions via the direct imposition method. Alternatively, and following earlier findings in statics (Terada et al., 2000; Van Der Sluis et al., 2000; Gitman et al., 2007), periodic boundary conditions are studied, which are here imposed using the so-called bipenalty method (see the Appendix for details). In Fig. 3 the results obtained with the two sets of boundary conditions are compared. It can be verified that the use of periodic boundary conditions has particular advantages in the determination of the averaged mass density. Therefore, in the remainder of the paper periodic boundary conditions will be used.

3.2. Effect of time-averaging

The present study evaluates the effectiveness of the space–time averaging method. To achieve this objective, we compare the averaged results of Young's modulus and mass density obtained by both space–time averaging and space averaging. To obtain the averaged material properties, a one-dimensional periodic laminated bar shown in Fig. 2, which enables comparisons with exact analytical solutions, is investigated under harmonic excitation with periodic boundary conditions, for the material contrast of $z_1/z_2 = 10$. The results of averaged Young's modulus and mass density are normalised by the analytical values given in Eqs. (17) and (18), respectively.

As shown in Fig. 4, the results of the space–time averaged material properties (i.e. $\langle\langle E_m\rangle_x\rangle_t$ and $\langle\langle \rho_m\rangle_x\rangle_t$) converge to those obtained by the analytical equivalents (i.e. E_{avr} and ρ_{avr}). Although the normalised macroscopic Young's modulus results obtained by the space averaging approach are reasonably accurate, those obtained by the space–time averaging approach converge considerably quicker and are fully consistent with the analytically averaged Young's modulus. On the other hand, the space averaging approach provides a poor estimation of the macroscopic mass density over time. Therefore, for dynamic multiscale problems, the use of space averaging may not be adequate. The space–time averaging approach generates reliable results for the macroscopic mass density as well as the macroscopic Young's modulus.

3.3. Effect of number of unit cells and number of wave propagations

With the superiority of periodic boundary conditions and space–time averaging established, the influence of number of unit cells N_{uc} and wave propagations N_{wp} along the bar on the averaged Young's modulus and averaged mass density can be investigated next. Most of the results converge progressively with increase in the number of unit cells and an ongoing propagation of the wave. While Fig. 5 shows the convergence of averaged Young's modulus, Fig. 6 shows mass density parameters in space and time, respectively. This analysis allows to find the best combination of those parameters since the computational effort required for doubling the number of unit cells is the same order of magnitude as for doubling the number of wave propagations.

The normalised results of Young's modulus shown in Fig. 5 converge with increasing N_{uc} and N_{wp}. The overriding observation is that a sufficient number of unit cells *as well as* a sufficient number of wave propagations is required to obtain accurate estimates for the macroscale material parameters.

Furthermore, the obtained space–time averaging results of Young's modulus and mass density do not appear to depend on the particular loading conditions, e.g. constant and harmonic loading conditions. As can be seen in Fig. 6, at the higher level impedance contrast, the results under constant load converge slightly quicker compared to harmonic load, but the overriding observation is that the influence of loading condition is relatively minor.

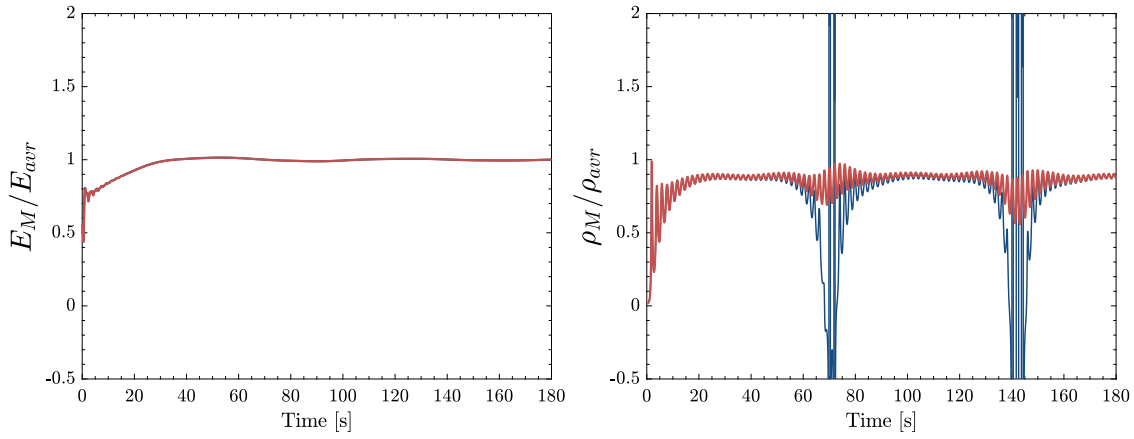

Fig. 3. Space–time averaging results of normalised averaged Young's modulus E_M/E_{avr} (left) and normalised averaged mass density ρ_M/ρ_{avr} (right). Comparisons between Dirichlet condition (blue line) and periodic boundary condition (red line) for the bar with material impedance contrast $z_1/z_2 = 100$ and constant excitation. (For interpretation of the references to colour in this figure legend, the reader is referred to the web version of this article.)

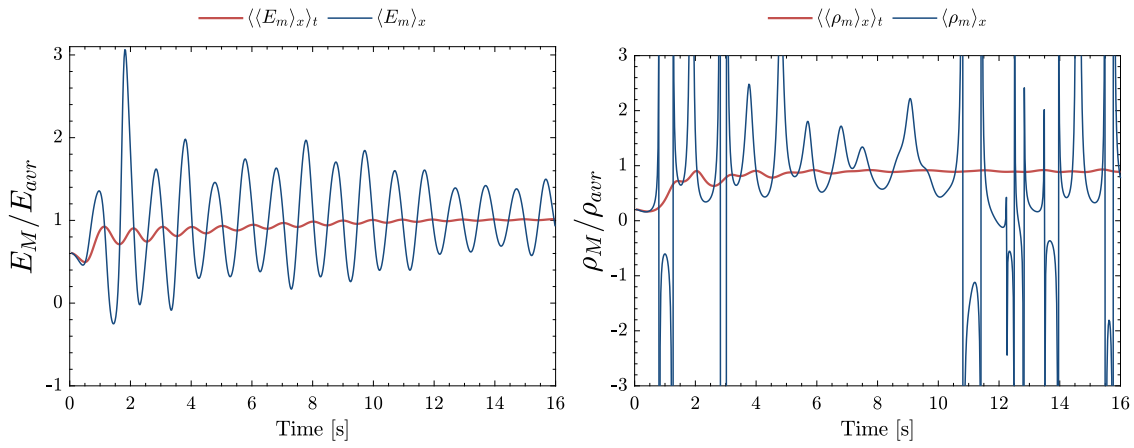

Fig. 4. Comparison of space and space–time averaging for normalised averaged Young's modulus E_M/E_{avr} (left) and normalised averaged mass density ρ_M/ρ_{avr} (right) where material impedance contrast is $z_1/z_2 = 10$ subjected to harmonic excitation with periodic boundary conditions.

3.4. Material parameter studies

Next, the numerical examples assess impedance contrasts between laminate components are assessed to ensure the robustness of the space–time averaging method. As can be seen in Figs. 5 and 6, accurate estimates of the macroscale material properties can still be obtained for increased impedance contrasts. Particularly, but not surprisingly, the averaged Young's modulus and mass density at the low-levels of impedance contrasts converge quicker than those at the medium and/or high-level impedance contrasts. Especially at higher levels of impedance contrasts, the most efficient approach is to aim simultaneously for a higher number of unit cells as well as a higher number of wave propagations to obtain accurate estimates for the macroscale parameters.

The influence of different volume fractions on the number of unit cells and wave propagations required to obtain converged macroscopic Young's modulus and mass density is investigated next. The bar is subjected to harmonic excitation with periodic boundary conditions, and the highest-level of impedance contrasts $z_1/z_2 = 1000$ in the material is considered. The volume fraction of the first component of the microscopic unit cell α is varied from 10% to 90%, while the macroscopic material parameters are estimated by simultaneously increasing the number of unit cells and wave propagations. For a wide range of volume fractions in the material, the macroscopic Young's modulus E_{M} and mass density ρ_{M} demonstrate good convergence with those obtained analytically at $N_{\text{uc}} = N_{\text{wp}} = 2^4$. The convergence performance of the macroscopic Young's modulus for the higher volume fractions of the first laminate is slower than that for the lower volume fractions, whereas the convergence performance of the macroscopic mass density for the higher volume fractions of the first laminate is faster than for lower volume fractions (see Fig. 7).

4. Conclusions

In this work, a new space and time averaging model between micro and macrostructure has been developed to obtain accurate estimates of macroscale material properties for elastodynamic multi-scale problems. In this context, the Hill–Mandel Principle is extended to include the effect of the time history on microstructure in addition to spatial heterogeneity. Therefore, in addition to the standard format of volume averaging, the time averaging leads to enhanced averaging relations between micro- and macrostructure.

To evaluate the validity of this averaging model, the response of a one-dimensional laminated bar with low, medium and high level impedance contrasts is investigated when subjected to several loading/boundary conditions. In particular, the averaged material parameters are analysed with the size of the microstructural sample and the time period of propagation of a longitudinal wave. Accordingly, this present model can be used to determine suitable RVE sizes in dynamic averaging problems. Whereas the results in the high level of impedance contrast is found to require larger RVE sizes and longer runtimes, the results for a low level of impedance contrast converge much quicker

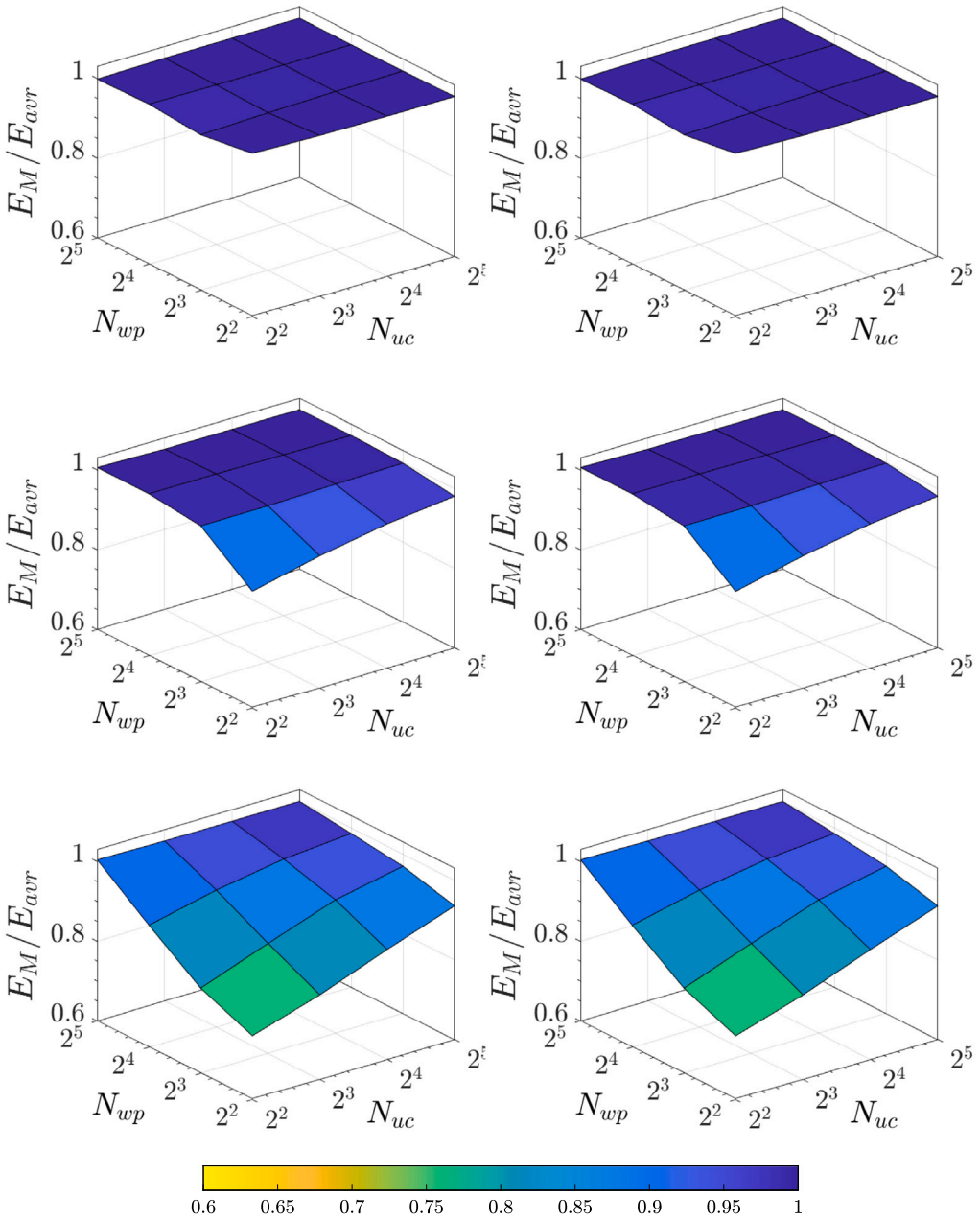

Fig. 5. Normalised averaged Young's modulus E_M/E_{avr} versus number of unit cells N_{uc} and number of wave propagations N_{wp} where material impedance contrasts are $z_1/z_2 = 10$ (top row), $z_1/z_2 = 100$ (middle row) and $z_1/z_2 = 1000$ (bottom row) subjected to constant (left column) and harmonic (right column) excitations.

— implying smaller RVE sizes and shorter runtimes. The numerical examples illustrate that a larger RVE size with shorter runtime can compensate for smaller RVE sizes with a longer runtime, and vice versa. The results of this paper may be used in other areas of mechanics that employ length scales, such as generalised continuum theories (gradient elasticity, gradient plasticity, etc.).

Declaration of competing interest

The authors declare that they have no known competing financial interests or personal relationships that could have appeared to influence the work reported in this paper.

Data availability

No data was used for the research described in the article.

Acknowledgement

İrem Yağmuroğlu gratefully acknowledges financial support by the Turkish Ministry of National Education Scholarship programme.

Appendix

Periodic boundary conditions

In this section, the equations of the bipenaly method (Hetherington et al., 2013) are presented to impose periodic boundary conditions on a one-dimensional periodic laminate bar. In the bipenalty method, displacement constraints are imposed together with the associated acceleration constraints for greater accuracy (and avoidance of problems

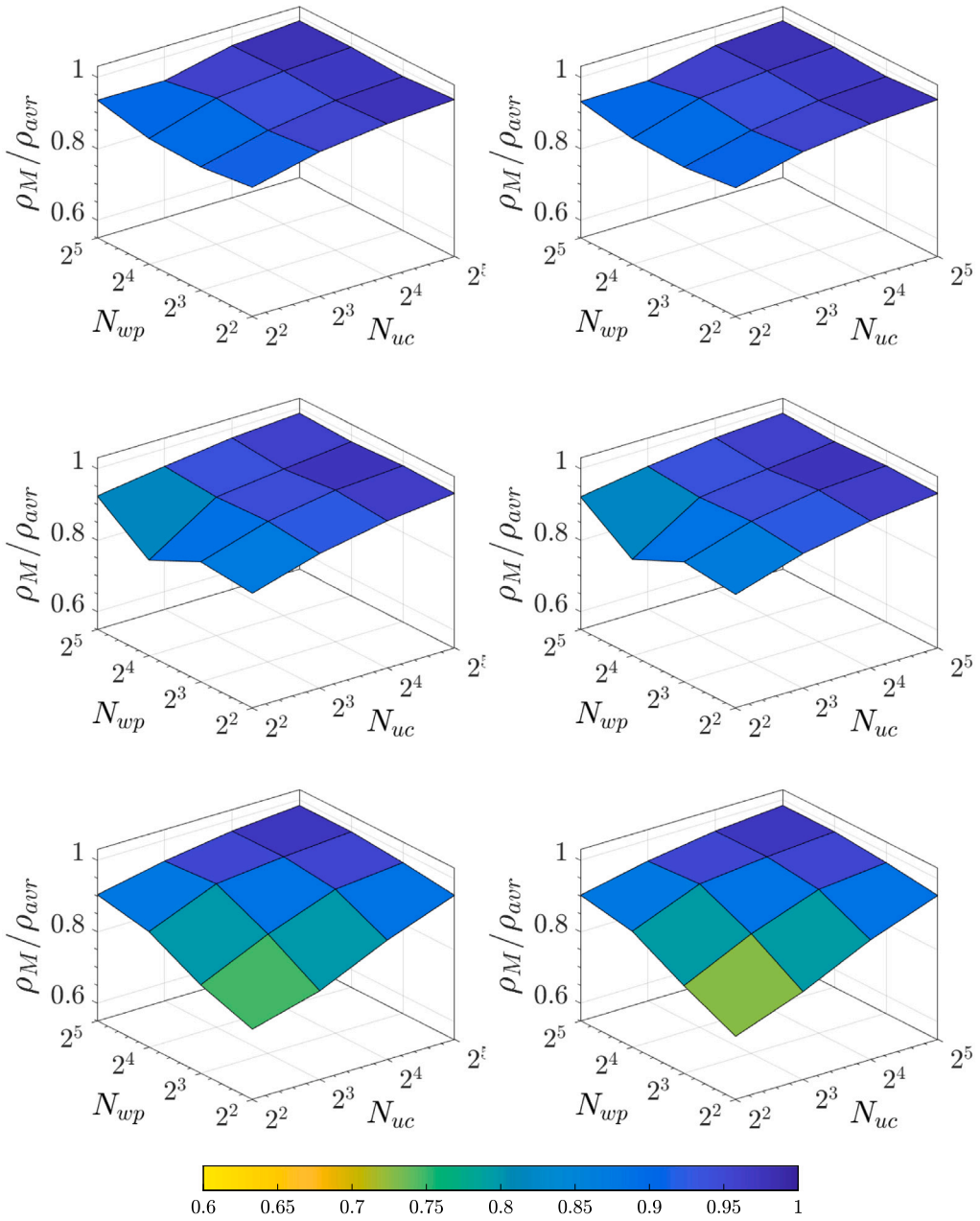

Fig. 6. Normalised averaged mass density ρ_M/ρ_{avr} versus number of unit cells N_{uc} and number of wave propagations N_{wp} where material impedance contrasts are $z_1/z_2 = 10$ (top row), $z_1/z_2 = 100$ (middle row) and $z_1/z_2 = 1000$ (bottom row) subjected to constant (left column) and harmonic (right column) excitations.

with stability). The matrix form of the equation of motion at the microscale Eq. (1) is given by

$$Mu + K\ddot{u} = 0 \tag{19}$$

where M and K are the mass matrix and stiffness matrix of the microstructure. In order to impose a tying between degrees of freedom with subscripts L and R, the equation of constraints for displacements (Askes et al., 2008) is written as

$$\bar{u} = u_{\mathrm{L}} - u_{\mathrm{R}} \tag{20}$$

where $\bar{u}$ is the prescribed displacements at the boundary of the microstructure. The displacement constraint is differentiated with respect to time to obtain the associated velocity constraint as follows

$$\dot{\bar{u}} = \dot{u}_{\mathrm{L}} - \dot{u}_{\mathrm{R}} \tag{21}$$

The contributions of Eqs. (20) and (21) in the potential $\mathscr{U}$ and kinetic energies $\mathscr{K}$ give

$$\mathscr{U} = \frac{1}{2}u^{\mathrm{T}}Ku + \frac{\alpha_{\mathrm{s}}}{2}(u_{\mathrm{L}} - u_{\mathrm{R}} - \bar{u})^2 \tag{22}$$

$$\mathscr{K} = \frac{1}{2}\dot{u}^{\mathrm{T}}M\dot{u} + \frac{\alpha_{\mathrm{m}}}{2}(\dot{u}_{\mathrm{L}} - \dot{u}_{\mathrm{R}} - \ddot{\bar{u}})^2 \tag{23}$$

where α_{s} and α_{m} are the stiffness and mass penalty parameters. Hence, the equation of motions can be derived in the following form

$$(M + M^{\mathrm{p}})\ddot{u} + (K + K^{\mathrm{p}})u = f^{\mathrm{p}} \tag{24}$$

where K^{p} is zero matrix except for the elements that imposing a tying between L and R, which are $K^{\mathrm{p}}{}_{\mathrm{LL}} = K^{\mathrm{p}}{}_{\mathrm{RR}} = \alpha_{\mathrm{s}}$ and $K^{\mathrm{p}}{}_{\mathrm{LR}} = K^{\mathrm{p}}{}_{\mathrm{RL}} = -\alpha_{\mathrm{s}}$. Similarly, $M^{\mathrm{p}}{}_{\mathrm{LL}} = M^{\mathrm{p}}{}_{\mathrm{RR}} = \alpha_{\mathrm{m}}$ and $M^{\mathrm{p}}{}_{\mathrm{LR}} = M^{\mathrm{p}}{}_{\mathrm{RL}} = -\alpha_{\mathrm{m}}$, whereas all other elements of M^{p} are zero. This leads to $f^{\mathrm{p}}{}_{\mathrm{L}} = -\alpha_{\mathrm{s}}\bar{u} - \alpha_{\mathrm{m}}\ddot{\bar{u}}$ and $f^{\mathrm{p}}{}_{\mathrm{R}} = \alpha_{\mathrm{s}}\bar{u} + \alpha_{\mathrm{m}}\ddot{\bar{u}}$, but all other elements of f^{p} are equal to zero.

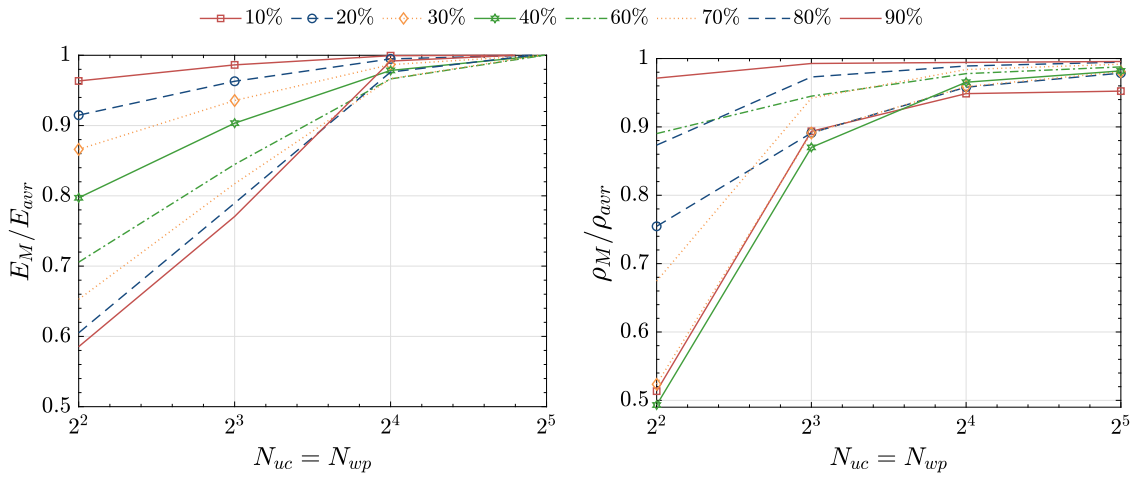

Fig. 7. Various volume fractions of components of periodic composites for normalised averaged Young's modulus E_M/E_{avr} (left) and normalised averaged mass density ρ_M/ρ_{avr} (right) where material impedance contrast is $z_1/z_2 = 1000$ subjected to harmonic excitation with periodic boundary conditions versus the same number of unit cells N_{uc} and wave propagations N_{wp}.

References

Andrianov, I.V., Bolshakov, V.I., Danishevs'kyy, V.V., Weichert, D., 2008. Higher order asymptotic homogenization and wave propagation in periodic composite materials. Proc. R. Soc. A 464, 1181–1201.

Askes, H., Piercy, S., Ilanko, S., 2008. Tyings in linear systems of equations modelled with positive and negative penalty functions. Commun. Numer. Methods. Eng. 24, 1163–1169.

Bagni, C., Gitman, I., Askes, H., 2015. A micro-inertia gradient visco-elastic motivation for proportional damping. J. Sound Vib. 347, 115–125.

Bennett, T., Gitman, I.M., Askes, H., 2007. Elasticity theories with higher-order gradients of inertia and stiffness for the modelling of wave dispersion in laminates. Int. J. Fract. 148, 185–193.

Chen, W., Fish, J., 2000. A dispersive model for wave propagation in periodic heterogeneous media based on homogenization with multiple spatial and temporal scales. J. Appl. Mech. 68 (2), 153–161.

de Souza Neto, E.A., Blanco, P.J., Sánchez, P.J., Feijóo, R.A., 2015. An RVE-based multiscale theory of solids with micro-scale inertia and body force effects. Mech. Mater. 80, 136–144.

Drugan, W.J., Willis, J.R., 1996. A micromechanics-based nonlocal constitutive equation and estimates of representative volume element size for elastic composites. J. Mech. Phys. Solids 44 (4), 497–524.

Fish, J., Chen, W., 2001. Higher-order homogenization of initial/boundary-value problem. J. Eng. Mech. 127, 1223–1230.

Fish, J., Filonova, V., Kuznetsov, S., 2012. Micro-inertia effects in nonlinear heterogeneous media. Internat. J. Numer. Methods Engrg. 91, 1406–1426.

Gitman, I.M., Askes, H., Aifantis, E.C., 2005. The representative volume size in static and dynamic micro-macro transitions. Int. J. Fract. 135, 3–9.

Gitman, I.M., Askes, H., Sluys, L.J., 2007. Representative volume: Existence and size determination. Eng. Fract. Mech. 74 (16), 2518–2534.

Gitman, I.M., Gitman, M.B., Askes, H., 2006. Quantification of stochastically stable representative volumes for random heterogeneous materials. Arch. Appl. Mech. 75, 79–92.

Hashin, Z., 1983. Analysis of Composite Materials — A Survey. J. Appl. Mech. 50 (3), 481–505.

Herakovich, C.T., 2012. Mechanics of composites: A historical review. Mech. Res. Commun. 41, 1–20.

Hetherington, J., Rodríguez-Ferran, A., Askes, H., 2013. The bipenalty method for arbitrary multipoint constraints. Internat. J. Numer. Methods Engrg. 93, 465–482.

Hill, R., 1963. Elastic properties of reinforced solids: Some theoretical principles. J. Mech. Phys. Solids 11 (5), 357–372.

Hill, R., 1972. On constitutive macro-variables for heterogeneous solids at finite strain. Proc. R. Soc. Lond. Ser. A Math. Phys. Eng. Sci. 326 (1565), 131–147.

Kanit, T., Forest, S., Galliet, I., Mounoury, V., Jeulin, D., 2003. Determination of the size of the representative volume element for random composites: statistical and numerical approach. Int. J. Solids Struct. 40 (13), 3647–3679.

Kanouté, P., Boso, D.P., Chaboche, J.L., Schrefler, B.A., 2009. Multiscale methods for composites: A review. Arch. Comput. Methods Eng. 16, 31–75.

Kouznetsova, V.G., Geers, M.G.D., Brekelmans, W.A.M., 2004. Multi-scale second-order computational homogenization of multi-phase materials: a nested finite element solution strategy. Comput. Methods Appl. Mech. Engrg. 193 (48–51), 5525–5550.

Nassar, H., He, Q.-C., Auffray, N., 2015. Willis elastodynamic homogenization theory revisited for periodic media. J. Mech. Phys. Solids 77, 158–178.

Nemat-Nasser, S., 1999. Averaging theorems in finite deformation plasticity. Mech. Mater. 31 (8), 493–523.

Nemat-Nasser, S., Hori, M., 2013. In: micromechanics: overall properties of heterogeneous materials, j. d. achenbach (eds.).

Nguyen, V.P., Lloberas-Valls, O., Stroeven, M., Sluys, L.J., 2011. Homogenization-based multiscale crack modelling: From micro-diffusive damage to macro-cracks. Comput. Methods Appl. Mech. Engrg. 200 (9), 1220–1236.

Ostoja-Starzewski, M., 2001. Microstructural randomness versus representative volume element in thermomechanics. J. Appl. Mech. 69 (1), 25–35.

Pham, K., Kouznetsova, V.G., Geers, M.G.D., 2013. Transient computational homogenization for heterogeneous materials under dynamic excitation. J. Mech. Phys. Solids 61 (11), 2125–2146.

Reina Romo, C., 2011. Multiscale Modeling and Simulation of Damage by Void Nucleation and Growth (Ph.D. thesis). California Institute of Technology.

Sheng, P., Chan, C.T., 2005. Classical wave localization and spectral gap materials. Z. Kristallogr. - Cryst. Mater. 220 (9–10), 757–764.

Sridhar, A., Kouznetsova, V.G., Geers, M.G.D., 2018. A general multiscale framework for the emergent effective elastodynamics of metamaterials. J. Mech. Phys. Solids 111, 414–433.

Sridhar, A., Kouznetsova, V.G., Geers, M.G.D., 2020. Frequency domain boundary value problem analyses of acoustic metamaterials described by an emergent generalized continuum. Comput. Mech. 65 (3), 789–805.

Srivastava, A., 2015. Elastic metamaterials and dynamic homogenization: a review. Int. J. Smart Nano Mater. 6 (1), 41–60.

Srivastava, A., Nemat-Nasser, S., 2014. On the limit and applicability of dynamic homogenization. Wave Motion 51 (7), 1045–1054.

Terada, K., Hori, M., Kyoya, T., Kikuchi, N., 2000. Simulation of the multi-scale convergence in computational homogenization approaches. Int. J. Solids Struct. 37, 2285–2311.

Van Der Sluis, O., Schreurs, P.J.G., Brekelmans, W.A.M., Meijer, H.E.H., 2000. Overall behaviour of heterogeneous elastoviscoplastic materials: Effect of microstructural modelling. Mech. Mater. 32, 449–462.

Wang, Z.-P., Sun, C.T., 2002. Modeling micro-inertia in heterogeneous materials under dynamic loading. Wave Motion 36 (4), 473–485.

Weinan, E., Engquist, B., Li, X., Weiqing, R., Vanden-Eijnden, E., 2007. Heterogeneous multiscale methods: A review. Commun. Comput. Phys. 2 (3), 367–450.

Willis, J.R., 1981. In: Yih, C.-S. (Ed.), Variational and Related Methods for the Overall Properties of Composites. In: Advances in Applied Mechanics, vol. 21, Elsevier, pp. 1–78.

Zhu, H.T., Zbib, H.M., Aifantis, E.C., 1997. Strain gradients and continuum modeling of size effect in metal matrix composites. Acta Mech. 121 (1), 165–176.